ISSN 2072-5981

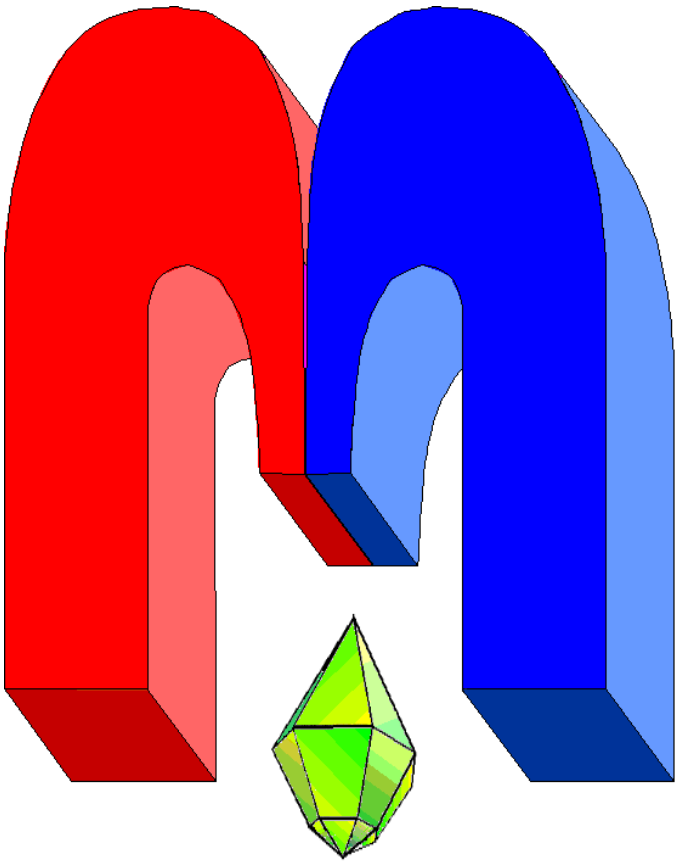

Magnetic Resonance in Solids

Electronic Journal

Volume ***19,***
Issue ***2***
Paper No ***17202,***
1-7 pages
2017

http://mrsej.kpfu.ru
http://mrsej.ksu.ru

Established and published by Kazan University
Sponsored by International Society of Magnetic Resonance (ISMAR)
Registered by Russian Federation Committee on Press, August 2, 1996
First Issue was appeared at July 25, 1997

"***Magnetic Resonance in Solids. Electronic Journal***" (**MRS*ej***) is a peer-reviewed, all electronic journal, publishing articles which meet the highest standards of scientific quality in the field of basic research of a magnetic resonance in solids and related phenomena.

Indexed and abstracted by
Web of Science (*ESCI*, Clarivate Analitics, from 2017), *Scopus* (Elsevier, from 2012), *RusIndexSC* (*eLibrary*, from 2006), *Google Scholar*, *DOAJ*, *ROAD*, *CyberLeninka* (from 2006), *SCImago Journal & Country Rank*, etc.

* In Kazan University the Electron Paramagnetic Resonance (EPR) was discovered by Zavoisky E.K. in 1944.

Spectral and magnetic properties of impurity Tm^{3+} ions in YF_3

A.V. Savinkov[1,*], G.S. Shakurov[2], I.E. Mumdzhi[1], B.Z. Malkin[1], S.I. Nikitin[1], S.L. Korableva[1], M.S. Tagirov[1,3]

[1] Kazan Federal University, Kremlevskaya 18, Kazan 420008, Russia

[2] Kazan Physical-Technical Institute, Sibirskiy trakt 10/7, Kazan 420029, Russia

[3] Institute of Perspective Research, TAS, L. Bulachnaya 36a, Kazan 420111, Russia

**E-mail: Andrey.Savinkov@gmail.com*

(Received November 27, 2017; accepted December 5, 2017)

Stark structure of $^3H_6$, $^3H_5$, $^3H_4$, $^3F_4$, $^3F_3$, $^3F_2$ and $^1G_4$ multiplets of impurity non-Kramers Tm^{3+} ions in the orthorhombic YF_3 crystal has been determined from luminescence studies. High frequency electron paramagnetic resonance (EPR) spectra (~207 GHz) of Tm^{3+} ions have been measured at temperature 4.2 K in external magnetic field applied perpendicular to the *b*-axis of YF_3:Tm^{3+} single crystal. The results of measurements are interpreted in the frameworks of the crystal field theory. The set of crystal field parameters related to the crystallographic system of coordinates of the YF_3 lattice has been obtained and used to reproduce satisfactory the crystal field energies and the EPR spectra.

PACS: 71.70.Ch, 71.70.Ej.

Keywords: crystal field parameters, exchange charge model, EPR, trifluorides

1. Introduction

The yttrium fluoride YF_3 crystals doped with heavy rare-earth ions (Sm, …, Tm and Yb) are investigated rather intensively because they may be suitable as potential solid-state laser materials and scintillators. Optical spectra of YF_3:R^{3+} and isostructural RF_3 (R = Eu, Tb, Dy, Er, Ho and Yb) crystals have been measured in Refs. [1-5]. Moreover, at present the rare-earth trifluorides attract more and more attention due to synthesis and investigation of magnetic and optical properties of the hollow fullerene-like nanoparticles RF_3 (R = La, Pr,…) and nanoparticles of different shapes [6-11] which can have widespread potential for practical applications in high resolution displays, electroluminescent devices and markers for biomolecules.

Fluoride TmF_3 and thulium doped YF_3 fluoride have been the subject of quite a few studies in the past. As a result, scanty information exists on magnetic properties of non-Kramers Tm^{3+} ions with the ground electronic configuration $4f^{12}$ in both concentrated, TmF_3, and dilute, YF_3:Tm^{3+}, compounds. Results of dc-magnetometry and NMR ^{19}F studies in TmF_3 powder as well as the high frequency electron paramagnetic resonance (EPR) measurements in YF_3:Tm^{3+} single crystal [12] gave unambiguous evidence that TmF_3 is a Van Vleck paramagnet with the gap $\Delta \sim 6.5$ cm^{-1} between the ground and the nearest excited energy levels of Tm^{3+} ions.

In present article we report the results of systematic studies of crystal field and magnetic properties of Tm^{3+} ions in YF_3:Tm^{3+} single crystal. The angular dependence of the high frequency EPR spectrum of Tm^{3+} ions was measured in the collinear constant ($\mathbf{B}_0$) and alternative ($\mathbf{B}_1$) magnetic fields lying in the crystallographic *ac*-plane ($\mathbf{B}_0 \parallel \mathbf{B}_1 \perp \mathbf{b}$). The Stark structure of electronic multiplets of Tm^{3+} ions was defined by means of the laser-selective spectroscopy. Crystal field parameters (CFP) were estimated in the frameworks of the semi-phenomenological exchange charge model [13] and then corrected by making use of our experimental data. The obtained set of CFP allowed us to reproduce satisfactory the high frequency EPR spectra in YF_3:Tm^{3+} single crystal.

2. Experimental data

The YF_3 : 0.5 at % Tm^{3+} single crystals for optical and EPR studies were grown by the Bridgman method in carbon crucibles in the atmosphere of the high purity argon at a pulling rate of 1 mm/h.

High purity TmF_3 and YF_3 powders (99,99% grade) were used as starting materials. Additionally, the growth atmosphere was fluorinated by thermal decomposition of the tetra-fluorine-ethylene.

2.1 Site-selective laser spectroscopy

Fluorescence of YF_3:Tm^{3+} crystal was excited with either a pulsed tunable dye laser (Littrow type oscillator and amplifier, linewidth of about 1 Å) pumped by the second or third harmonic of a Nd-YAG laser (LQ129, Solar LS) in the visible spectral range or a Ti:Sapphire tunable laser with the linewidth of about 0.4 Å (LX325, Solar LS) pumped by the second harmonic of a Nd-YAG laser (LQ829, Solar LS) in the near-IR range. The spectra were analyzed with an MDR-23 monochromator. The fluorescence signal was detected by a cooled photomultiplier (PMT-106 or PMT-83) in the photon-counting mode. The studied YF_3:Tm^{3+} crystal was kept in the helium vapor at a temperature of 4.2 K. In order to investigate fluorescence spectra at temperatures about 2 K liquid helium bath cryostat with the vapor pumping was used.

We studied the fluorescence of the YF_3:Tm^{3+} crystal corresponding to the radiative transitions from the metastable states of the Tm^{3+} ions, namely, from the lowest crystal field sublevels of the $^1G_4$ and $^3F_4$ multiplets, to the low-lying multiplets $^3H_6$, $^3H_5$ and $^3H_4$ ($^1G_4 \rightarrow {}^3H_6$, $^1G_4 \rightarrow {}^3H_5$, $^1G_4 \rightarrow {}^3H_4$ and $^3F_4 \rightarrow {}^3H_6$). Energies of the crystal field sublevels of the ground ($^3H_6$) and low lying excited ($^3H_5$ and $^3H_4$) multiplets were determined from the selectively excited luminescence spectra (see luminescence spectra for $^1G_4 \rightarrow {}^3H_6$ and $^3F_4 \rightarrow {}^3H_6$ in Fig. 1a).

Energies of crystal field sublevels of the $^3F_4$, $^3F_3$, $^3F_2$ and $^1G_4$ multiplets were determined from the excitation spectra of Tm^{3+} ions in YF_3 host. The first excited sublevel of the ground multiplet $^3H_6$ (see Table 1) is separated from the ground sublevel by the energy of 6.5 cm^{-1}. At temperature $T = 4.2$ K both sublevels are populated. Hence, excitation spectra arise due to transitions from the both lowest

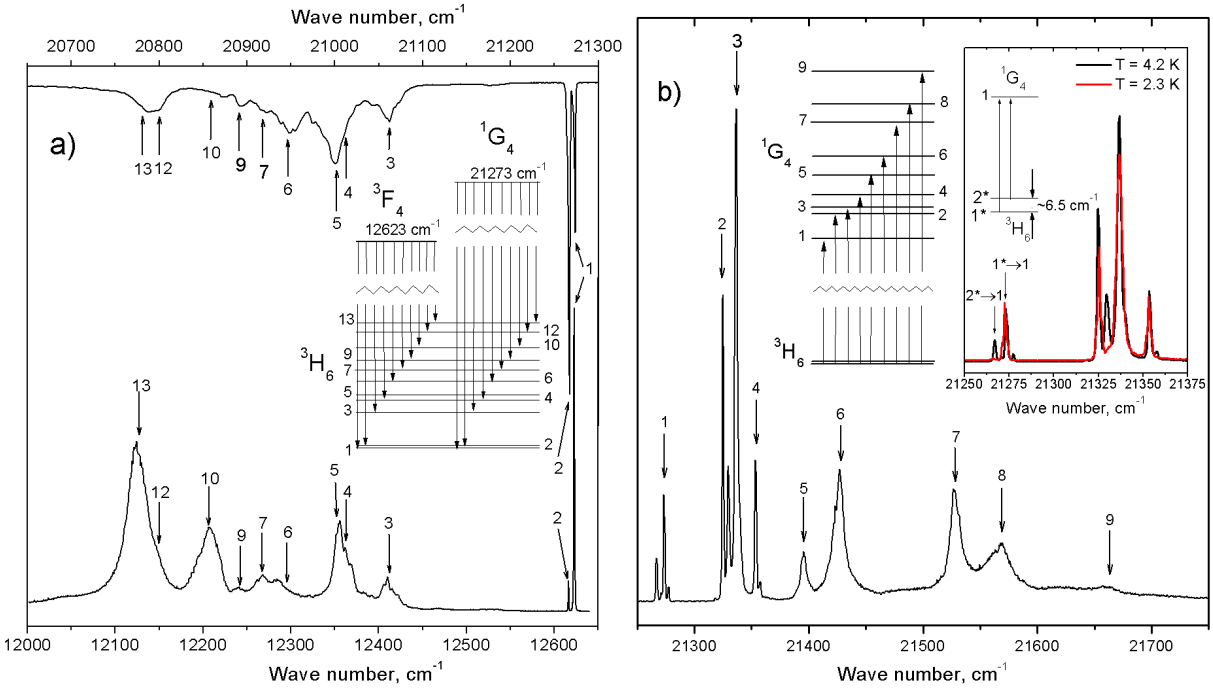

Figure 1. (a) Luminescence spectra of Tm^{3+} ions measured in YF_3:Tm^{3+} at $T = 4.2$ K. The emission from the lowest sublevels of $^3F_4$ (lower spectrum) and $^1G_4$ (upper spectrum) multiplets into the sublevels of the ground $^3H_6$ multiplet was induced by radiation with the wave numbers of 12959.1 cm^{-1} and 21424.7 cm^{-1}, respectively. (b) The excitation spectrum of the Tm^{3+} ions in YF_3:Tm^{3+} corresponding to transitions from the lowest states of $^3H_6$ into the $^1G_4$ at 4.2 K. The inset shows the difference between the excitation spectra measured at $T = 4.2$ K (black curve) and $T = 2.3$ K (red curve) due to redistribution of populations of the ground quasi-doublet sublevels.

sublevels of the $^3H_6$ multiplet to sublevels of the $^3F_4$, $^3F_3$, $^3F_2$ and $^1G_4$ multiplets. As a result, spectral lines registered at $T = 4.2$ K are split by the energy 6.5 cm^{-1} (see the transition $^3H_6 \rightarrow {}^1G_4$ in Fig. 1b). In order to determine the crystal field energies of the $^1G_4$ and $^3F_2$ multiplets, the excitation spectra of Tm^{3+} ions corresponding to the transitions from the ground state into the $^1G_4$ and $^3F_2$ multiplets at lower temperature $T = 2.3$ K were measured (see inset in Fig. 1b). Crystal field energies for $^3H_6$, $^3H_5$, $^3H_4$, $^3F_4$, $^3F_3$, $^3F_2$ and $^1G_4$ multiplets of Tm^{3+} ions obtained from the analysis of the experimental data are presented in Tab. 1.

Table 1. Crystal field energies (cm^{-1}) of the Tm^{3+} ions in YF_3 host.

$^{2S+1}L_J$	N	Experiment	Calculation
$^3H_6$	1	0	0
	2	6.5	6.5
	3	212	211
	4	262	265
	5	274	277
	6	326	327
	7	356	354
	8	-	367
	9	381	398
	10	417	420
	11	-	435
	12	475	473
	13	499	482
$^3H_4$	1	5800	5803
	2	5825	5834
	3	5860	5856
	4	5886	5884
	5	5904	5904
	6	-	5910
	7	5960	5967
	8	5981	5981
	9	-	6065
$^3H_5$	1	8263	8257
	2	8270	8264
	3	8448	8446
	4	8468	8478
	5	8510	8510
	6	8557	8553
	7	-	8581
	8	8603	8589
	9	8643	8592
	10	8650	8615
	11	8659	8624
$^3F_4$	1	12623	12622
	2	12684	12683
	3	-	12764
	4	12792	12794
	5	-	12835
	6	12853	12852
	7	12871	12873
	8	12940	12932
	9	12959	12952
$^3F_3$	1	14555	14558
	2	14625	14619
	3	14629	14628
	4	14649	14646
	5	14654	14650
	6	14685	14666
	7	14752	14717
$^3F_2$	1	15208	15184
	2	15227	15216
	3	15237	15232
	4	15329	15330
	5	-	15355
$^1G_4$	1	21273	21261
	2	21325	21291
	3	21336	21349
	4	21353	21353
	5	21395	21390
	6	21425	21428
	7	21527	21530
	8	21568	21549
	9	21660	21652

2.2 High frequency EPR in YF_3:Tm^{3+}

The EPR spectra of Tm^{3+} ions in oriented YF_3:Tm^{3+} (0.5% Tm) single crystal were taken with high-frequency tunable EPR spectrometer [14] at frequency of 207 GHz in magnetic fields from 0 to 900 mT at temperature 4.2 K. The microwave magnetic field $\mathbf{B}_1$ was applied parallel to static magnetic field $\mathbf{B}_0$, i.e. $\mathbf{B}_1 \parallel \mathbf{B}_0$. The hyperfine structure of the EPR spectra consisting of two resonant lines was observed (Fig. 2a). This observation gives evidence for resonance transitions induced by the microwave field in Tm^{3+} ions (^{169}Tm, $I = 1/2$, natural abundance 100%).

High-frequency EPR spectra measured in the YF_3:Tm^{3+} single crystal allowed us to determine the energy gap of 6.5 cm^{-1} between the two lowest crystal field singlets. The magnetic moments corresponding to this quasi-doublet are determined by the *g*-factor ~13.5 and lie in the *ac*-plane along the directions declined by the angle ~ ±23° from the crystallographic *c*-axis [12]. The angular dependence of the EPR spectrum was measured by rotation of a sample around the crystallographic *b*-axis so that the external magnetic field was applied in the *ac*-plane of the YF_3 crystal lattice, the angular step in the *ac*-plane was 5°. Two magnetically non-equivalent sites of Tm^{3+} ions were found. EPR spectra in the magnetic fields lying in the *ab*-plane were not observed because the resonant field was out of the magnetic field range for our magnet. Some of EPR lines are distorted, split, and have weak satellites. Probable reasons for these effects were discussed in Ref. [12].

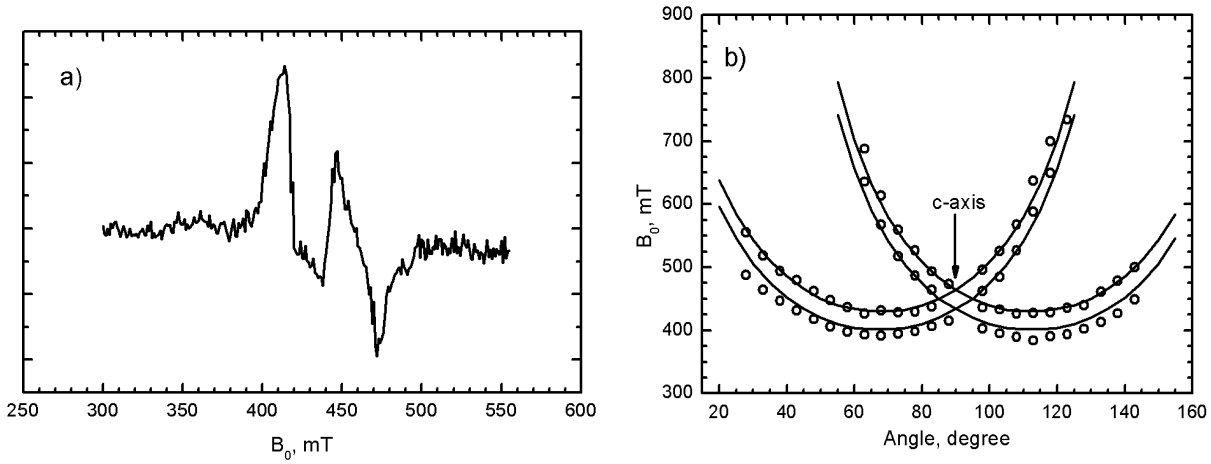

Figure 2. The high frequency EPR (207 GHz) of Tm^{3+} ions measured in YF_3:Tm^{3+} single crystal: (a) a sample spectrum of the Tm^{3+} EPR, measured at $\mathbf{B}_0\hat{}\mathbf{a} = 48°$; (b) the angular dependence measured in external magnetic field applied in the *ac*-plane of YF_3 crystal structure. Open circles and solid lines represent the experimental data and the calculated resonant magnetic fields, respectively.

3. Discussion

The single crystals YF_3:Tm^{3+} studied in this work have an orthorhombic structure with the space group *Pnma* (D_{2h}^{16}) [15]. The lattice constants are $a = 0.63537(7)$ nm, $b = 0.68545(7)$ nm, $c = 0.43953(5)$ nm [16]. The unit cell contains four formula units. The coordinates of fluorine F1 ions in 4c positions and F2 ions in 8d positions are determined by parameters u_1, u_2, s_2, v_1, v_2 and equal $\pm(u_1, 1/4, v_1)$, $\pm(u_1 - 1/2, 1/4, 1/2 - v_1)$ for F1, $\pm(u_2, s_2, v_2)$, $\pm(u_2, 1/2 - s_2, v_2)$, $\pm(u_2 - 1/2, s_2, 1/2 - v_2)$, $\pm(u_2 - 1/2, 1/2 - s_2, 1/2 - v_2)$ for F2; the yttrium ions in 4c positions with the point symmetry C_s have the coordinates $\pm(u, 1/4, v)$, $\pm(u - 1/2, 1/4, 1/2 - v)$. The fractional parameters u_1, v_1, u_2, s_2, v_2, u, v (in units of the lattice constants) in YF_3 [16] that is used as a host matrix for Tm^{3+} ions are represented in Tab. 2.

To describe the results of EPR and optical measurements, we consider the effective Hamiltonian of a single Tm^{3+} ion in the *j*-sublattice, operating in the total basis of 182 electron-nuclear states of the electronic $4f^{12}$ configuration, in the external magnetic field $\mathbf{B}_0$:

Table 2. Fractional atomic coordinates of the ions in *Pnma* structure of YF_3 [16].

Y		F1		F2		
u	v	u_1	v_1	u_2	s_2	v_2
0.3673(4)	0.0591(5)	0.5227(5)	0.5910(8)	0.1652(4)	0.0643(3)	0.3755(5)

$$H_j = H_0 + H_{\mathrm{CF},j} + H_{\mathrm{HF}} + H_{\mathrm{Z},j} \,. \tag{1}$$

Here H_0 is the free ion Hamiltonian defined by Slater parameters $F^2 = 102586$ cm^{-1}, $F^4 = 72072$ cm^{-1}, $F^6 = 51572$ cm^{-1} of electrostatic interaction between 4f-electrons, spin-orbit coupling constant $\xi = 2634.5$ cm^{-1}; two-particle parameters of the configuration interaction, parameters of correlated spin-orbit and spin-spin interactions were taken from Ref. [17]. The term H_{HF} is the energy of the magnetic hyperfine interaction:

$$\begin{aligned} H_{\mathrm{HF}} = A\sum_n \{ & \mathbf{l}_n\mathbf{I} + \sqrt{3/2}[2C^{(2)}_{0,n}\left(3s_{n,z}I_z - \mathbf{s}_n\mathbf{I}\right)/\sqrt{6} + \\ & + \left(C^{(2)}_{2,n} + C^{(2)}_{-2,n}\right)\left(s_{n,x}I_x - s_{n,y}I_y\right) - i\left(C^{(2)}_{2,n} - C^{(2)}_{-2,n}\right)\left(s_{n,x}I_y + s_{n,y}I_x\right) - \\ & - \left(C^{(2)}_{1,n} - C^{(2)}_{-1,n}\right)\left(s_{n,x}I_z + s_{n,z}I_x\right) + i\left(C^{(2)}_{1,n} + C^{(2)}_{-1,n}\right)\left(s_{n,z}I_y + s_{n,y}I_z\right)]\} . \end{aligned} \tag{2}$$

Here $A = 2\mu_{\mathrm{B}}\gamma_{\mathrm{Tm}}\hbar\left\langle r^{-3}\right\rangle_{4\mathrm{f}}$ is the hyperfine coupling constant, where μ_{B} is the Bohr magneton, $\gamma_{\mathrm{Tm}}/2\pi = 3.52$ MHz/T is the gyromagnetic ratio for ^{169}Tm nuclei, $\mathbf{l}_n$ and $\mathbf{s}_n$ are the orbital and spin moments, respectively, of 4f-electrons; $C^{(2)}_{q,n}$ are the electronic spherical tensor operators and $\mathbf{I}$ is the nuclear spin moment. The average value of $1/r^3$ for 4f-electrons defines the effective hyperfine constant that is taken as $A = -0.016$ cm^{-1}. The sum is taken over all 4f-electrons.

The electronic Zeeman energy is $H_{\mathrm{Z},j} = -\boldsymbol{\mu}\mathbf{B}_{0,j}$, where $\boldsymbol{\mu} = -\mu_{\mathrm{B}}\sum_n(\mathbf{l}_n + 2\mathbf{s}_n)$ is the electronic magnetic moment of the Tm^{3+} ion. The Tm^{3+} ions in the sublattices $j = 1$ and 2, 3 and 4 are magnetically equivalent in pairs.

The crystal field Hamiltonian

$$H_{\mathrm{CF},j} = \sum_{k=2,4,6}\sum_{q=0:k} B^k_q(j)\sum_n O^q_{n,k} \,, \tag{3}$$

in the Cartesian system of coordinates defined so that $x \| c$, $y \| b$ and $z \| a$, is determined by a single set of 15 crystal field parameters (CFP) $B^k_q(1)$ $(B^k_q(1) = B^k_q(2) = (-1)^k B^k_q(3) = (-1)^k B^k_q(4))$, $O^q_{n,k}$ are linear combinations of spherical tensors defined in Ref. [18].

Initial values of CFP for the Tm^{3+} ions in YF_3 (column "Calculated" in Tab. 3) were calculated in the framework of the exchange charge model [13] by making use of the corresponding lattice structure constants and atomic coordinates presented above in Tab. 2:

$$B^k_q = \sum_L e^2[-Z_L(1-\sigma_k)\langle r^k\rangle + \frac{2(2k+1)}{7}R^k_L S_k(R_L)](-1)^q C^{(k)}_{-q}(\vartheta_L, \varphi_L)/R^{k+1}_L \,. \tag{4}$$

In the expression (4), the sum is taken over lattice ions L with charges eZ_L and spherical coordinates (R_L, ϑ_L, φ_L) relative to the rare earth ion at the origin, σ_k are the shielding constants, $\langle r^k\rangle$ are the moments of the 4f-electron charge density, the exchange charges are defined by the overlap integrals between the wave functions of the rare earth ions $\left|4\mathrm{f}, l_z\right\rangle$ and ligand ions $\left|l, l_z\right\rangle$ (we take into account only the outer closed $2s^2$ and $2p^6$ electronic shells of F^- ions) [13]:

$$S_k(R_L) = G_s S_s^2(R_L) + G_\sigma S_\sigma^2(R_L) + \gamma_k G_\pi S_\pi^2(R_L), \quad (5)$$

where $S_S = \langle 4f\,0 | 2s\,0 \rangle$, $S_\sigma = \langle 4f\,0 | 2p\,0 \rangle$, $S_\pi = \langle 4f\,1 | 2p\,1 \rangle$ and $\gamma_2 = -\gamma_6 = 3/2$, $\gamma_4 = 1/3$.

Calculations were carried out with $\sigma_2 = 0.545$, $\sigma_4 = 0.088$, $\sigma_6 = -0.043$ [19], $\langle r^2 \rangle = 0.646$, $\langle r^4 \rangle = 1.076$, $\langle r^6 \rangle = 3.647$ (atomic units) [20], the dependences of the overlap integrals on the distance R (in Angstrems) between the ions were approximated by functions $S_0 \exp(-bR^d)$ with the parameters $S_0 = 0.33789$, 0.19678, 2.93065; $b = 1.52924$, 1.48051, 0.8624; $d = 1.05503$, 0.81048, 2.93065 for s, σ and π bonds, respectively [21]. The values of the model parameters were assigned as $G_s = G_\sigma = G_\pi = 11.5$. Hereafter, the calculated values of CFP (see column "Calculated" in Tab. 3) were corrected to fit the measured electronic energies of Tm^{3+} ions in YF_3. The final set of the CFP is represented in Tab. 3 (column "Adjusted").

The calculated crystal field energies of the $^3H_6$, $^3H_5$, $^3H_4$, $^3F_2$, $^3F_3$, $^3F_4$, $^1G_4$ multiplets of Tm^{3+} ion in YF_3 host are compared with the experimental data in Tab. 1. The total splittings of the excited multiplets and energies of the most sublevels are well reproduced by calculations (see Tab. 1, column "Calculation"). The standard deviation of the calculated values of crystal field energies from those experimentally defined is STD ~ 14 cm^{-1}.

The obtained set of CFP allowed us to reproduce satisfactory the angular dependence of the Tm^{3+} EPR spectrum (Fig. 2b). The calculated principal value of the g-factor for the lowest quasi-doublet equals $g = 13.59$, the corresponding principal direction lies in the *ac*-plane and has the angle φ of ±22.0° with the *c*-axis of YF_3 crystal. These calculated values are close to experimental data, $g = 13.5$ and $\varphi = \pm 23.0°$.

Table 3. The crystal field parameters (in cm^{-1}) of the Tm^{3+} ions in YF_3 crystal lattice.

B_q^k	Calculated	Adjusted
B_0^2	103	117
B_1^2	838	802
B_2^2	–264	–306
B_0^4	–1.76	–3.45
B_1^4	–711	–584
B_2^4	–11.9	–3.46
B_3^4	289	210
B_4^4	97.3	83.4
B_0^6	–0.90	–1.0
B_1^6	–309	–261
B_2^6	–303	–185
B_3^6	–43.4	–32.4
B_4^6	–77.5	–65.3
B_5^6	–923	–896
B_6^6	265	237

4. Conclusion

The crystal field energies of the impurity Tm^{3+} ions in orthorhombic crystal YF_3 have been determined for $^3H_6$, $^3H_5$, $^3H_4$, $^3F_4$, $^3F_3$, $^3F_2$, and $^1G_4$ multiplets from the optical absorption and luminescence studies. The initial set of crystal field parameters for the Tm^{3+} ions in the YF_3 host has been calculated in the framework of the semi-phenomenological exchange charge model and then varied to fit the experimental data. The obtained set of CFPs allowed us to reproduce well the electronic energies and the angular dependence of EPR spectra measured in YF_3:Tm^{3+} single crystal in external magnetic fields applied in the *ac*-plane. The calculated value and the direction of the magnetic moment of the Tm^{3+} ion in the ground quasi-doublet state agree well with the results of EPR measurements.

Acknowledgments

This work was supported by the RFBR grant №15-02-06990_a.

References

1. Caspers H.H., Rast H.E., Fry J.L. *J. Chem. Phys.* **47**, 4505 (1967)
2. Kuroda H., Shionoja S., Kushida T. *J. Phys. Soc. Jpn.* **33**, 125 (1972)

3. Bumagina L.A., Kazakov B.N., Malkin B.Z., Stolov A.L. *Phys. Solid State* **19**, 624 (1977) (*Fizika Tverdogo Tela* **19**, 1073 (1977), *in Russian*)
4. Davidova M.P., Kazakov B.N., Stolov A.L. *Phys. Solid State* **20**, 1378 (1978) (*Fizika Tverdogo Tela* **20**, 2391 (1978), *in Russian*)
5. Sharma K.K., Spedding F.H., Blinde D.R. *Phys. Rev. B* **24**, 82 (1981)
6. Ma L., Chen W.-X., Zheng Yi-F., Zhao J., Xu Zh. *Materials Letters* **61**, 2765 (2007)
7. Wang X., Li Y.D. *Chem. Eur. J.* **9**, 5627 (2003)
8. Alakshin E.M., Klochkov A.V., Kondratyeva E.I., Korableva S.L., Kiiamov A.G., Nuzhina D.S., Stanislavovas A.A., Tagirov M.S., Zakharov M.Yu, Kodjikian S. *Journal of Nanomaterials* **2016**, 7148307 (2016)
9. Alakshin E.M., Gazizullin R.R., Klochkov A.V., Korableva S.L., Safin T.R., Safiullin K.R., Tagirov M.S. *Opt. Spectrosc.* **116**, 721 (2014)
10. Alakshin E.M., Blokhin D.S., Sabitova A.M., Klochkov A.V., Klochkov V.V., Kono K., Korableva S.L., Tagirov M.S. *JETP letters* **96**, 194 (2012)
11. Gazizulina A.M., Alakshin E.M., Baibekov E.I., Gazizullin R.R., Zakharov M.Yu., Klochkov A.V., Korableva S.L., Tagirov M.S. *JETP Letters* **99**, 149 (2014)
12. Savinkov A.V., Shakurov G.S., Korableva S.L., Dooglav A.V., Tagirov M.S., Suzuki H., Matsumoto K., Abe S. *J. Phys.: Conf. Series* **324**, 012033 (2011)
13. Malkin B.Z. *Spectroscopy of Solids Containing Rare-Earth Ions*, ed. by Kaplyanskii A.A. and Macfarlane R.M., Elsevier Science Publishers, Amsterdam (1987)
14. Tarasov V.F., Shakurov G.S. *Appl. Magn. Reson.* **2**, 571 (1991)
15. Zalkin A., Templeton D.H. *J. Am. Chem. Soc.* **75**, 2453 (1953)
16. Cheetham A.K., Norman N. *Acta Chemica Scandinavica A* **28**, 55 (1974)
17. Carnall W.T., Goodman G.L., Rajnak K., Rana R.S. *J. Chem. Phys.* **90**, 3443 (1989)
18. Klekovkina V.V., Zakirov A.R., Malkin B.Z., Kasatkina L.A. *J. Phys. Conf. Series* **324**, 012036 (2011)
19. Sternheimer R.M., Blume M., Peierls R.F. *Phys. Rev.* **173**, 376 (1968)
20. Abragam A., Bleaney B. *Electron Paramagnetic Resonance of Transition Ions*, Clarendon Press, Oxford (1970)
21. Aminov L.K., Malkin B.Z., *Dynamics and Kinetics of Electronic and Spin Excitations in Paramagnetic Crystals*, KFU Press, Kazan (2008) (*in Russian*)